f-State Occupancy at the γ-α Phase Transition of Ce-Th and Ce-Sc Alloys

J.-P. Rueff,[1] C. F. Hague,[1,2] J.-M. Mariot,[1] L. Journel,[1] R. Delaunay,[1] J.-P. Kappler,[3,2] G. Schmerber,[3] A. Derory,[3] N. Jaouen,[4] and G. Krill[2]

[1]*Laboratoire de Chimie Physique–Matière et Rayonnement (UMR 7614), Université Paris 6, 11 rue Pierre et Marie Curie, 75231 Paris Cedex 05, France*
[2]*LURE, Centre Universitaire Paris Sud, Bâtiment 209 D, BP 34, 91898 Orsay Cedex, France*
[3]*IPCMS (UMR 7504), 23 rue du Lœss, BP 43, 67034 Strasbourg Cedex, France*
[4]*ESRF, BP 220, 38043 Grenoble Cedex, France*

(Received 19 December 2003; published 4 August 2004)

Resonant inelastic x-ray scattering spectra were measured for a series of Ce solid solutions (Ce-Th and Ce-Sc) across the γ-α phase transition. They reveal a well-defined feature associated with the $4f^2$ configuration when the incident energy is tuned to the Ce L_3 preedge region. This component is normally hidden in x-ray absorption spectra because of lifetime broadening. The f^1/f^2 ratio estimated by resonant inelastic x-ray scattering presents a sharp drop across the γ-α transition and hysteresis as a function of temperature that closely resemble the magnetization loop. These measurements confirm recent dynamical mean-field theory calculations that unexpectedly predict significant double occupancy of f orbitals in the ground state.

DOI: 10.1103/PhysRevLett.93.067402 PACS numbers: 78.70.En, 71.20.Eh, 71.27.+a

The Ce γ-α transition is one of the most intriguing phenomena in condensed matter physics. It embraces a variety of complex mechanisms generating anomalous behavior both on a structural level (lattice parameter), and, more fundamentally, in the magnetic (magnetization) and electronic properties (specific heat, etc.). There is a solid consensus even beyond the widely discussed Mott transition [1] and the Kondo volume collapse paradigms [2,3] that hybridization between $4f$ and valence electrons plays a key role in the phase transition. Hybridization may be defined formally in terms of configuration interaction. Then, the ground state is written as a linear combination of $|4f^0v^{n+1}\rangle$, $|4f^1v^n\rangle$, and $|4f^2v^{n-1}\rangle$ electronic states (v stands for the valence electrons), i.e., in terms of unoccupied, singly, or doubly occupied f states, respectively. In particular, the large Ce γ-α volume collapse ($\Delta V/V_0 \approx 14\%$) is supposedly driven by a change in interactions involving f orbitals. A precise estimate of the relative weight of these electronic configurations across the phase transition is of prime interest in this respect.

First-principles calculations ranging from the self-interaction-corrected local-spin-density approach [4] to dynamic mean-field theory (DMFT) allied to the local-density approximation (LDA) (LDA + DMFT) [5,6] have proved to be powerful methods for calculating the ground-state properties of Ce in both the γ and α phases. However, there are nontrivial disparities between them regarding electron interactions (see Ref. [6]) and, over the years, various spectroscopic methods have also been put forward to help clarify them. Ce L-edge x-ray absorption spectroscopy (XAS) should be the privileged technique because under the influence of the f electron core-hole Coulomb interaction, U_{fc}, it is possible to separate the mainly $|\underline{2p}4f^0v^{n+2}\rangle$ and $|\underline{2p}4f^1v^{n+1}\rangle$ final states (underscore means a hole state). Yet, since the seminal work of Gunnarsson and Schönhammer [7,8], it is largely accepted that the presence of a core hole in the XAS final state rules out extracting the ground-state occupation number directly from the XAS data. In particular, any sign of preedge structure attributable to the f^2 configuration is difficult to extract.

It has been demonstrated recently that L-edge resonant inelastic x-ray scattering (RIXS) applied to the rare earths provides detailed information on the f electronic properties [9–11]. In RIXS, the final-state electron count is the same as in the initial state, i.e., $|4f^mv^n\rangle \rightarrow |\underline{2p}4f^mv^{n+1}\rangle \rightarrow |\underline{3d}4f^mv^{n+1}\rangle$ with $m = 0, 1, 2$ and $m + n = \text{const}$. A resonance observed below the L edge indicates better screening of the core hole. Screening by an extra valence electron would be at the expense of f-state occupancy and would give a poorly screened core-hole state that resonates above the edge. Thus, preedge structure is necessarily attributed to screening by an extra f electron because U_{fc} is large. Such a structure is reached by electric dipole transitions but involves $|\underline{2p}4f^2v^n\rangle$ intermediate states [10]. We show that RIXS may be discussed on a par with x-ray photoelectron spectroscopy (XPS). Fuggle *et al.* [12] pointed out that Ce $3d$ XPS yields information relevant to the ground state properties. However, the XPS surface sensitivity tends to artificially reinforce the Ce-γ character, though recently Jung *et al.* have claimed that this may be circumvented in Ce by high-energy XPS [13]. In contrast to XPS, RIXS is a true bulk probe and is well suited to address the γ-α transition problem.

The γ-α transition is normally triggered by applying external pressure, but the transition may also be tracked as a function of temperature by using chemical pressure [14] such as substituting Th or Sc for Ce. The formation of the parasitic β phase observed in Ce at normal pressures is avoided and sample handling is simplified. In this Letter, we apply Ce $2p3d$ RIXS to Ce-Th and Ce-Sc solid solutions which exhibit a comparable γ-α transition. By tuning the incident-photon energy to the Ce L_3 preedge, we were able to observe f^2-related states, hidden in XAS, and follow the evolution of the f^1/f^2 ratio as the temperature was cycled through the γ-α transition. The f double occupancy is shown to have a sizable weight in both γ and α phases. The results provide a critical test for theoretical models of correlated f electron systems.

The experiment was carried out on the ID12 beam line at the European Synchrotron Radiation Facility [15]. Polycrystalline ingots of $Ce_{0.93}Sc_{0.07}$, $Ce_{0.90}Th_{0.10}$, and $Ce_{0.80}Th_{0.20}$ were prepared by triarc melting in the presence of a Zr oxygen getter and under purified argon atmosphere. Homogeneity was obtained by remelting 10 times for a weight loss of less than 0.5%. The structure was checked by x-ray diffraction. Freshly scraped samples were mounted in our x-ray Raman spectrometer [16] operated at $<10^{-7}$ mbar. No changes due to oxidation were observed in the course of the measurements.

The inset to Fig. 1 shows Ce L_3 XAS data measured in the total fluorescence-yield mode for $Ce_{0.90}Th_{0.10}$. The spectra at 300 and 60 K are indistinguishable. The intense white line peak at 5728.8 eV and the very weak feature at ≈ 5736 eV are, respectively, ascribed to the mainly $\underline{2p}4f^1$ and $\underline{2p}4f^0$ components. It is noteworthy that no changes in the preedge region are visible as the temperature is driven through the γ-α transition. We will see that RIXS is far more sensitive to the γ-α transition.

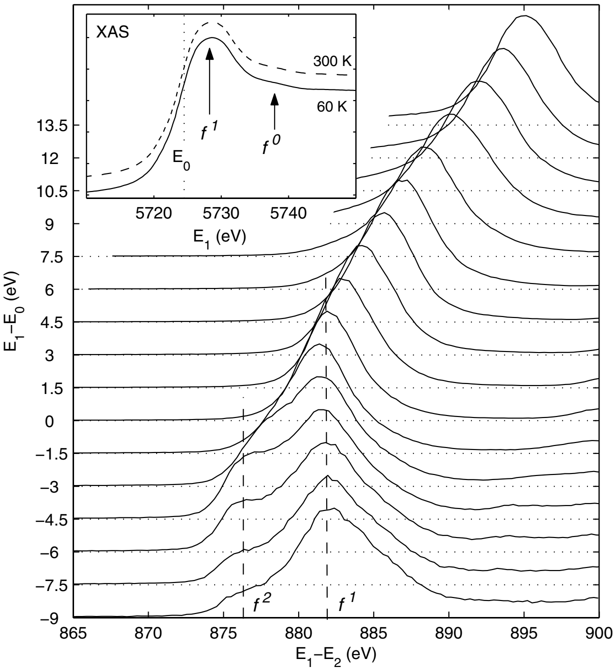

FIG. 1. Ce $2p3d$ RIXS spectra for $Ce_{0.90}Th_{0.10}$ at 60 K as a function of the transfer energy. The RIXS maximum amplitude is normalized to unity and spectra are offset for clarity. The incident energies are indicated on the left scale, relative to the edge position E_0 shown in the inset. The dashed lines indicate the RIXS components attributed to the mainly $\underline{3d}4f^25d^n$ and $\underline{3d}4f^15d^{n+1}$ final states. Inset: total fluorescence-yield XAS spectrum at 60 and 300 K.

RIXS spectra for $Ce_{0.90}Th_{0.10}$ taken at 60 K are shown in Fig. 1 on a transfer energy scale ($E_1 - E_2$) where the incident and scattered photon energies are E_1 and E_2, respectively. Similar results were obtained for the two other samples. Here, we focus on the $L\alpha_1$ spectral region. In the figure, incident energies are given relative to the L_3-edge inflection point E_0 ($= 5724.5$ eV; see the inset). We can distinguish two opposite behaviors depending on the incident energy: In the preedge region ($E_1 - E_0 < 0$), the RIXS spectra appear at constant transfer energy indicating the Raman regime; in contrast, the dispersion of the RIXS spectra above threshold ($E_1 - E_0 > 0$) denotes the onset of the fluorescence regime. The Raman spectra have a double peak structure. The peak at 881.9 eV transfer energy resonates close to the white line energy and corresponds to the $\underline{3d}4f^15d^{n+1}$ final state. The peak at 876.1 eV resonates well below the edge and is assigned to the better screened $\underline{3d}4f^25d^n$ state. The 5.8 eV energy separation is less than U_{fc} ($\approx$ 11–13 eV) because f-f and valence-to-core Coulomb interactions also intervene.

The resonance enhancement due to the RIXS process allows us to precisely determine the variation of the f^1/f^2 ratio with temperature as it is cycled through the γ-α transition. Figure 2 shows the temperature dependence of the RIXS spectra in $Ce_{0.90}Th_{0.10}$ measured at fixed incident energy $E_1 - E_0 = -6$ eV. The spectra are arbi-

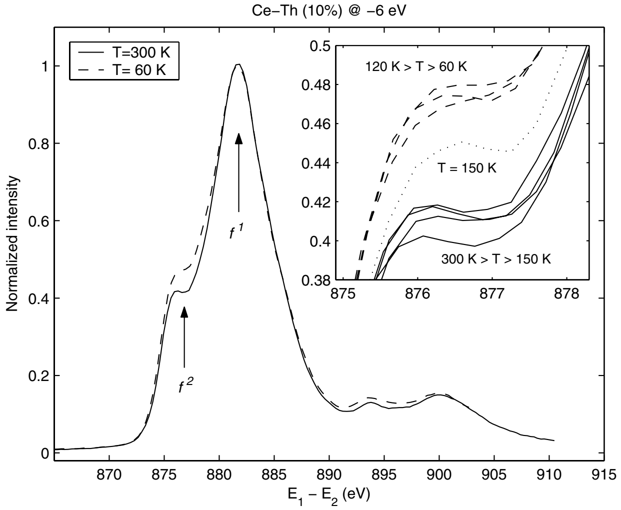

FIG. 2. Variation of the Ce $2p3d$ RIXS spectra measured at a fixed incident energy, 6 eV below the Ce L_3 edge, in $Ce_{0.90}Th_{0.10}$, while changing the temperature through the γ-α transition. The spectra were normalized to maximum amplitude. The f^2 region is enlarged in the inset.

trarily normalized to the f^1 intensity. The f^2 shoulder shows a marked relative increase in intensity when the temperature is lowered below the transition; i.e., f^1/f^2 is extremely sensitive to the temperature change. This is presented in Fig. 3 where we show the temperature dependence of the f^1/f^2 intensity ratio in the three samples. All three samples show a sharp decrease at the transition temperature and hysteresis that point to a first-order transition. The hysteresis depends on the concentration of the alloying element; the width of the loop ranges from 10 K in $Ce_{0.80}Th_{0.20}$ to 55 K in $Ce_{0.90}Th_{0.10}$ and 85 K in $Ce_{0.93}Sc_{0.07}$.

In Fig. 3 we compare the RIXS data analysis to the hysteresis loop obtained from magnetization curves taken with a field $H = 2$ T for the same samples. Obviously the magnetization is a ground-state property whereas RIXS involves excited final states. Even so, the striking resemblance between the two sets of data is not coincidental and underlines the intimate relationship between the RIXS data and the anomalous behavior at the γ-α transition. The concentration dependence of the hysteresis loop is also reminiscent of dilatometry measurements [14], another ground-state property. In the latter case, the width of the hysteresis is largest in pure Ce and shrinks with chemical substitution, similarly to our observation going from panels (c) to (a) in Fig. 3.

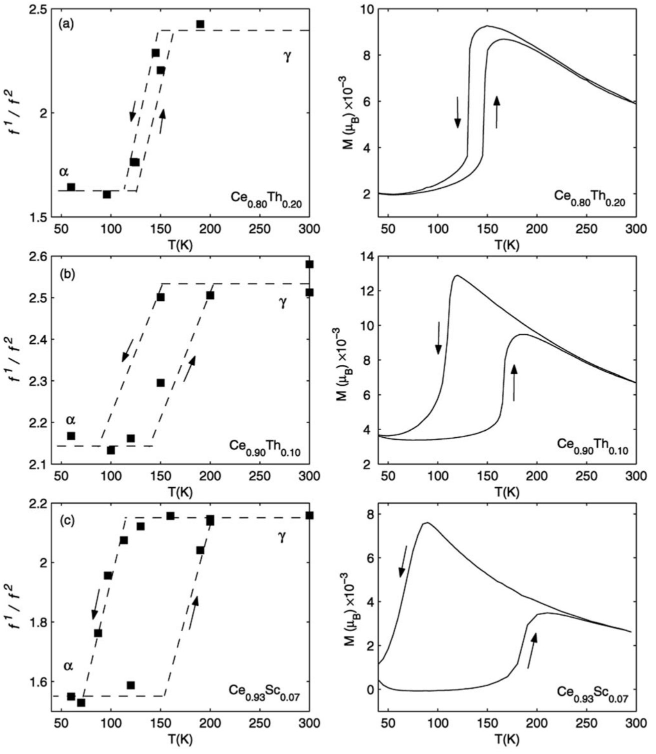

FIG. 3. Left panels: variation of the f^1/f^2 intensity ratio derived from the RIXS data analysis in (a) $Ce_{0.80}Th_{0.20}$, (b) $Ce_{0.90}Th_{0.10}$, and (c) $Ce_{0.93}Sc_{0.07}$, as the temperature is cycled through the γ-α transition. The arrows indicate the circulation inside the loop. Right panels: magnetization at $H = 2$ T in the same samples as a function of temperature. To be noticed is the close resemblance between the two series of measurements in spite of their different nature.

McMahan *et al.* [6] predict that the weight of doubly occupied states increases at the expense of single occupancy when the system goes from γ to α: At the γ-α transition, the Ce-Ce interatomic distance dramatically shrinks, which strengthens the f itinerant character through hybridization. This is confirmed by the RIXS data in Fig. 3 where we observed a decrease of the f^1/f^2 ratio at low temperature. Note that the f^1/f^2 ratios as they appear in Figs. 2 and 3 strongly overestimate the f^2-related states because the RIXS intensity in the f^2 spectral region is partly due to a tail excitation of the f^1-related states. To extract the correct f^1/f^2 intensity ratio from the RIXS spectra, we applied the phenomenological model that we developed in Ref. [10]. The model simulates the RIXS spectra by using semielliptical density of states to represent the f^1- and f^2-related contributions (see Fig. 4) and taking into account the finite width of the Gaussian excitation function and the Lorentzian-like core-hole broadening effect in the intermediate and final states. The RIXS spectra are calculated at each excitation energy by the overlap between the Lorentzian functions and the excitation, weighted by the density of states. The widths, amplitudes, and energy positions of the model f^1 and f^2 semiellipses are adjusted to fit the data. Once these have been set, the complete series of spectra is simulated consistently by changing E_1 only.

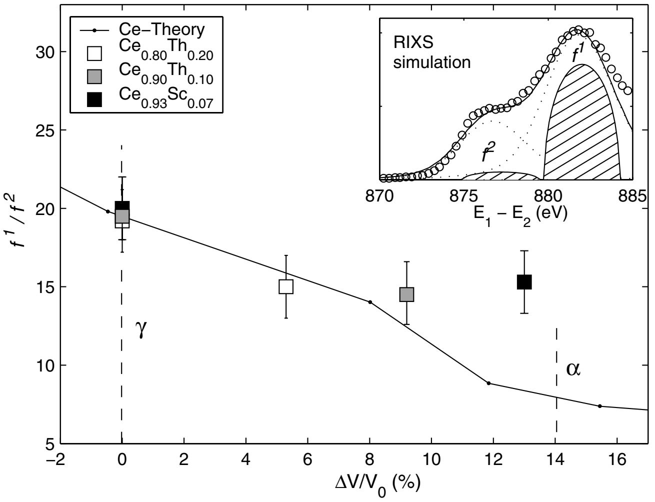

FIG. 4. f^1/f^2 ratio derived from the RIXS simulation (squares) as a function of the relative volume change, compared to the theoretical calculations in pure Ce from Ref. [6] (dots). Inset: experimental (open circles) and simulated RIXS (solid line) spectra in $Ce_{0.90}Th_{0.10}$ at 60 K. The hatched areas represent the f^1 and f^2 model density of states, and the dotted lines their contribution to the RIXS spectrum.

TABLE I. Estimated volume change and f^1/f^2 ratios derived from RIXS analysis (see the text for details) in Ce solid solutions.

	Sample	$\Delta V/V_0$[a]	f^1/f^2 intensity ratio α phase	γ phase
RIXS	$Ce_{0.80}Th_{0.20}$	5.0%	15.0	19.2
	$Ce_{0.90}Th_{0.10}$	9.2%	14.9	19.5
	$Ce_{0.93}Sc_{0.07}$	12.3%	15.3	20.0
Theory[b]	Pure Ce	14.0%	7.9	19.6

[a] From Ref. [14].
[b] From Ref. [6].

As underlined in Ref. [7], the relative weights of the f^n peaks in the final state of various spectroscopies are modified relative to the ground state due to changes in hybridization. However, in the Raman regime when the excitation is tuned specifically to the f^2-related states, the dipole transition is dominated by their strong overlap with f^2 ground states. Thus the weight of the f^2 structure in the RIXS spectrum is mainly determined by the ground state f^2-state occupancy and not by hybridization with the $\underline{3d}4f^15d^{n+1}$ states, considering that f^2 final states are well below the f^1 states (5.8 eV), and the Raman process is faster than the intermediate state relaxation (this is no longer valid in the fluorescence regime). On the other hand, the weight of the f^1 final states is very much dominant in these alloys, so it will be only weakly affected in the RIXS final state by the change in hybridization with the f^2 states. This explains that the f^1/f^2 ratios measured here are expected to track the ground state values quite closely and can be used to validate the calculated values. Table I summarizes the results for the three samples either side of the γ-α transition from the RIXS simulation. The results are compared to the theoretical predictions for pure Ce given in Ref. [6].

The ratio of singly to doubly occupied states is ≈ 20 in the γ phase for all the samples. This confirms the calculated value. In the α phase the experimental f^1/f^2 ratio is more than a factor of 2 higher than the calculation for pure Ce. In Ce-Th, such a discrepancy can be explained by the smaller volume contraction (see Table I) compared to Ce: At a larger volume the f electrons are still largely correlated and the sample less α-like, hence a larger intensity ratio. When renormalized to the volume change, the calculations of McMahan *et al.* would equate to a ratio of 17.2 and 15.2 for α-$Ce_{0.90}Th_{0.10}$ and α-$Ce_{0.80}Th_{0.20}$, respectively. This is consistent with our estimate, considering the moderate precision of the calculations and uncertainties of our RIXS simulations (see the error bars in Fig. 4). Ce-Sc on the contrary undergoes a volume change comparable to Ce, though the f^1/f^2 ratio in the α phase differs significantly from that of the pure metal. We can tentatively interpret this in terms of the difference in hybridization with the Sc $3d^1$ valence states compared to Th with its nominally $6d^2$ configuration. In view of the apparent success of LDA + DMFT calculations in predicting hybridization effects at the Ce γ-α transition it is hoped they can be extended to such alloys in disordered solid solutions.

In conclusion, the f^1/f^2 ratio measured by RIXS as a function of temperature scales both with ground-state properties such as magnetization and the occupation numbers derived from state-of-the-art first principles calculations. We believe that, thanks to resonant enhancement and bulk sensitivity, RIXS provides unequivocal information not readily obtained by the other techniques, namely, XPS because of surface effects and XAS because of experimental broadening and, for energies above the white line, artifacts due to relaxation.

Note added.—A preprint by Dallera *et al.* [17] referring to a similar experimental work has come to our attention just prior to publication.

[1] B. Johansson, Philos. Mag. **30**, 469 (1974).
[2] J.W. Allen and R.M. Martin, Phys. Rev. Lett. **49**, 1106 (1982).
[3] M. Lavagna, C. Lacroix, and M. Cyrot, Phys. Lett. **90A**, 210 (1982).
[4] Z. Szotek, W.M. Temmerman, and H. Winter, Phys. Rev. Lett. **72**, 1244 (1994).
[5] M.B. Zölfl *et al.*, Phys. Rev. Lett. **87**, 276403 (2001).
[6] A.K. McMahan, K. Held, and R.T. Scalettar, Phys. Rev. B **67**, 075108 (2003).
[7] O. Gunnarsson and K. Schönhammer, Phys. Rev. B **28**, 4315 (1983).
[8] O. Gunnarsson *et al.*, Phys. Rev. B **28**, 7330 (1983).
[9] J.-M. Mariot *et al.*, Physica (Amsterdam) **259B–261B**, 1136 (1999).
[10] L. Journel *et al.*, Phys. Rev. B **66**, 045106 (2002).
[11] C. Dallera *et al.*, Phys. Rev. Lett. **88**, 196403 (2002).
[12] J.C. Fuggle *et al.*, Phys. Rev. B **27**, 7330 (1983).
[13] R.J. Jung *et al.*, Phys. Rev. Lett. **91**, 157601 (2003).
[14] K.A. Gschneider, R.O. Elliott, and R.R. McDonald, J. Phys. Chem. Solids **23**, 1191 (1962).
[15] J. Goulon *et al.*, Physica (Amsterdam) **208B–209B**, 199 (1995).
[16] C.F. Hague *et al.*, J. Electron Spectrosc. Relat. Phenom. **110–111**, 179 (2000).
[17] C. Dallera *et al.*, Phys. Rev. B (to be published).